



# High latitude, dayside ULF signals observed from ground in Greenland

Marie Vigger Eldor <sup>1</sup>, Magnar Gullikstad Johnsen <sup>2</sup>, Nils Olsen <sup>1</sup>, and Anna Naemi Willer <sup>1</sup>

<sup>1</sup>Division of Geomagnetism and Geospace, DTU Space, National Space Institute, Technical University of Denmark, Akademivej 356, 2800 Kgs. Lyngby, Denmark

Correspondence: Marie Vigger Eldor (marvig@space.dtu.dk)

Abstract. Ultra-low frequency (ULF) waves propagate through the cusp and generate distinct summertime signatures in high latitude ground-based magnetometer measurements. In this study, we apply four years of data from the high time resolution West Greenland magnetometer chain and perform a statistical analysis of ULF signal distribution as a function of season, magnetic latitude, magnetic local time, and interplanetary magnetic field parameters. We find that ULF signals at the highest latitudes, in the cusp and beyond, are sensitive to seasonal change, indicating that the ionospheric currents that generate the signal depend on solar illumination to obtain sufficient conductivities. This effect, in concert with dipole tilt, is investigated, and a clear cusp-related ULF signal population during summer was found. In winter, this population merges with other ULF signals associated with Alfvénic interhemispheric bouncing further south and thus disappears. Earlier studies, which have mainly been performed during winter conditions, failed to unambiguously identify cusp ULF signals. Furthermore, we discuss other aspects of our statistical analysis and briefly address implications for other known cusp phenomena.

### 1 Introduction

20

*Ultra low frequency* (ULF) signals have been studied extensively using ground-based magnetometers over the last century (e.g., Eschenhagen, 1897; Rolf, 1931; Harang, 1932, and many to come). The *International Geophysical Year* (1958–59) saw a tremendous increase in reports of geomagnetic pulsations, and soon thereafter, the *International Association of Geomagnetism and Aeronomy* (IAGA) put forward a scheme (Jacobs et al., 1964) for their classification into continuous (Pc) and irregular (Pi) pulsations. Pc and Pi are further divided into numbered subcategories according to the frequency bands: Pc 1 (200–5000 mHz), Pc 2 (100 – 200 mHz), Pc 3 (22.2 – 100 mHz), Pc 4 (6.67 – 22.2 mHz), Pc 5 (1.67 – 6.67 mHz), Pi 1 (25 – 1000 mHz), Pi 2 (6.67 – 25 mHz). With the advent of the space age, satellites could verify the magnetospheric origins of the magnetic signatures on the ground (e.g., Sonett et al., 1959; Greenstadt et al., 1967; Heppner et al., 1967; Sonnerup et al., 1969).

Substorm studies have established a clear relationship between Pi 2 signatures and substorm onset. These are waves that are generated in relation to the westward travelling surge that propagates across *magnetic local times* (MLTs) and thus have a global signature (Sakurai and McPherron, 1983; Kepko and Kivelson, 1999). The review paper by Glassmeier (1989) details ULF distribution and occurrence as a function of latitude and MLT; however, due to low sampling and poor data coverage, only a limited amount of high-latitude studies have been conducted. One of these is the study by Rostoker et al. (1972)

<sup>&</sup>lt;sup>2</sup>Tromsø Geophysical Observatory (TGO), UiT the Arctic University of Norway, 9037 Tromsø, Norway

https://doi.org/10.5194/egusphere-2025-5396 Preprint. Discussion started: 14 November 2025





30



who investigated the occurrence of Pc 4 and Pc 5 pulsations throughout Canada  $(58.7^{\circ} - 77.7^{\circ})$  magnetic latitudes). They found one population of narrow-band ULF signals in the cusp vicinity that increased in frequency with decreasing magnetic latitude, which is consistent with an Alfvén wave bouncing between the hemispheres on closed field lines. Furthermore, another wideband ULF population was discovered north of  $\sim$ 75° magnetic latitude that was attributed to processes in the polar cusp, and thus they suggested it could be used as a proxy for the *open closed fieldline boundary* (OCB).

McHarg and Olson (1992) and McHarg et al. (1995) were the first to associate observed dayside, broadband ULF waves with auroral particle precipitation at cusp latitudes from Svalbard. They proposed a categorisation based on daily changes in the cusp signature as the observing station rotates with the Earth. This was later challenged by Engebretson et al. (1995), who applied the *magnetometer array for cusp and cleft studies* (MACCS) network of search coil magnetometers to show that the signatures observed by McHarg et al. (1995) occur simultaneously over a large portion of the dayside, high latitude, ionosphere. In a more recent study Pilipenko et al. (2015) used SuperDARN data to show how ULF signals occur several degrees lower than the polar cusp location, further supporting the findings of Engebretson et al. (1995). However, due to the lack of high-latitude climatological studies of the ULF signal occurrence, its origin is still not fully established.

Although dayside observations of ULF waves have been studied for many years, the bulk of work has been focused on wintertime cusp dynamics and magnetic latitudes up to  $75^{\circ}$ . Owing to the general inaccessibility on the ground to magnetic latitudes above  $\sim 75^{\circ}$ , fewer studies, using the MACCS magnetometer network and the *Automated Geophysical Observatories in Antarctica* (e.g., Engebretson et al., 2006), have focused on very high latitudes. E.g. Vennerstrøm (1999), performed a statistical study of Pc 5 signals using the Greenland magnetometer chain. Recent upgrades enhance the potential of the Greenland magnetometers as a high cadence, dense magnetometer chain available for statistical investigations of ULF waves below these frequencies, covering auroral oval to polar cap latitudes.

In this paper, we present statistical results of ULF wave activity from the Greenland magnetometer chain, with a focus on covering magnetic latitudes from the auroral zone to the polar cap. We found the existence of a distinct population of ULF wave activity equatorward and poleward of the statistical cusp region, with a clear minimum separating it from the region of ULF waves associated with dynamics along the auroral oval, on closed field lines. After presenting the used data and their processing in Sect. 2, we report on the results in Sect. 3 and discuss them in relation to potential driving mechanisms, magnetospheric dynamics, and other parameters such as solar wind in Sect. 4. The paper finishes with a conclusion and outlook in Sect. 5.

#### 2 Data and data processing

We use 1-second magnetometer data from the four years 2020–2023 obtained from ground stations along the west coast of Greenland. The *quasi-dipole* (QD) latitude and longitude (Richmond, 1995) of the stations, listed in Table 1, show that the stations cover auroral, cusp, and polar cap regions. We extract the magnetic signal in the ULF range, denoted as  $X_{ULF}$ , by applying a Butterworth bandpass filter (10-600 s period corresponding to Pc 3–5 and Pi 2) to the northward component X. With this approach, we will not be able to make a distinction between discrete or broadband ULF signals, but rather their average strength. Since the bandpass filter returns all magnetic signals within the chosen frequency band, we here use the





Table 1. West Greenland magnetometer chain with corresponding QD-coordinates and MLT noon times computed for 2024.

Location	Station code	<b>QD-latitude</b> (°)	<b>QD-longitude</b> (°)	MLT noon (UT hours)
Qaanaaq	THL	83.50	22.63	15:38
Pituffik Space Base	TAB	82.63	21.69	15:44
Savissivik	SVS	81.79	27.18	15:23
Kullorsuaq	KUV	79.53	36.59	14:45
Upernavik	UPN	77.70	35.75	14:51
Uummannaq	UMQ	75.11	38.70	14:40
Qeqertarsuaq	GDH	73.90	35.99	14:53
Attu	ATU	72.59	35.12	14:57
Kangerlussuaq	STF	71.24	37.86	14:45
Maniitsoq	SKT	69.95	34.62	15:00
Nuuk	GHB	68.47	35.40	14:57
Paamiut	FHB	65.85	36.82	14:52
Narsarsuaq	NAQ	64.20	40.89	14:34

terminology "signal/signature" when referring to the magnetic response of a ULF wave measured at a ground magnetometer station.

To ensure continuity and avoid spurious zero values caused by the bandpass filtering, we apply a 10-minute moving average to  $|X_{ULF}|$  to obtain  $[|X_{ULF}|]_{10}$ , where "10" denotes the 10-minute moving average. Later, an averaged version of  $[|X_{ULF}|]_{10}$  denoted  $\overline{[|X_{ULF}|]_{10}}$  is used, calculated by averaging over four years.

#### 3 Results

70

Figure 1 (a)–(d) shows four years of  $[|X_{ULF}|]_{10}$  for the four stations, from north to south, THL, UPN, STF, and NAQ. They are approximately located along the same magnetic meridian on the west coast of Greenland. The panels are plotted with respect to MLT and time of year; the colour code indicates the strength of the ULF signal. In Fig. 1 (e), we display the *ap* index. Since this index attempts to describe global geomagnetic activity without a local longitude component, we display it using universal time on the vertical axis. Figure 1 (f) displays the daily average ULF signal at THL and solar zenith angle at magnetic noon, as well as F10.7 solar flux.

At THL in the polar cap, a ULF signature centred around magnetic local noon is observed during the summer months, with increasing amplitude as F10.7 increases, displaying a clear solar cycle dependence. The seasonal variation in  $[|X_{ULF}|]_{10}$  is anti-correlated with that of the solar zenith angle. At UPN, a similar but slightly stronger ULF signature is found around



75



magnetic local noon, but of smaller seasonal variation compared to THL. At both THL and UPN, dominant ULF signals across all MLTs occur simultaneously during increased values of *ap*, suggesting a relation to global geomagnetic activity.

Moving to the auroral latitudes, ULF signals at STF are seen both at night and during the day. The nighttime ULF signals are likely due to geomagnetic storms and substorm activity, as supported by the *ap* index seen in Fig. 1 (e). The ULF signals at daytime span from 4 to 16 MLT and increase in amplitude with F10.7, indicative of a solar irradiance dependence, with the highest amplitudes during dawn. Furthermore, a weak local minimum is seen around noon. Some of the daytime signals at STF occur during high *ap*, displaying a strong ULF response to geomagnetic storms. During times with low *ap* values, the daytime signal is not as prominent at STF, setting it apart from the daytime signals at THL and UPN, which occur independently of geomagnetic storms.

At NAQ, in the southern part of the auroral zone, the majority of the ULF signals occur during nighttime, likely associated with substorm activity. However, daytime ULF signals occur during times of increased *ap* values and become more frequent as F10.7 increases, further indicating an association with geomagnetic storms.

The average ULF amplitudes,  $\overline{[|X_{ULF}|]_{10}}$ , during summer (May to July) as a function of MLT and QD-latitude are displayed in Fig. 2 for different IMF clock angles. Equatorward and poleward boundaries of the Feldstein model (Feldstein and Starkov, 1967; Holzworth and Meng, 1975) of the statistical auroral oval are shown by blue, resp. green, curves (computed for activity Q=3). At  $\sim 73^{\circ}$  QD-latitude, a ULF signal occurs during daytime for all clock angles as observed by several stations. It is mainly located on the dayside within the boundaries of the statistical auroral oval, i.e., on closed magnetic field lines, and amplified for IMF  $B_z < 0$ , suggesting a relation to subsolar reconnection or enhanced energy transfer to the ionosphere. The relation between high ap values and dayside ULF signals at STF is supported by Fig. 1 panels (c) and (e). Nightside ULF signals related to substorm activity are seen at QD-latitudes 65–75° during all clock angles but noticeably amplified for IMF  $B_z < 0$ .

Poleward of the statistical auroral oval (red curves in Fig. 2), a strong ULF signal occurs in the 8–16 MLT time interval during all IMF clock angles. This indicates that ULF signals here are generated by sources not directly associated with substorm activity, but rather with direct, dayside solar wind magnetosphere interaction and dynamics on open magnetic field lines. Furthermore, the ULF amplitudes are more dominant in the dawn (dusk) sector during IMF  $B_y < 0$  ( $B_y > 0$ ), indicating that the high-latitude dayside ULF signal is controlled by processes in the solar wind independent of IMF  $B_z$  but adjusted by IMF  $B_y$ .

Figure 3 displays the 10-minute average ULF amplitude as a function of MLT and QD-latitude divided into seasons. During summer (Fig. 3 (c)), two separate ULF populations are seen, one poleward of 75° QD-latitude and one southward of 75° QD-latitude, as is also seen in Fig. 2. However, during winter (Fig. 3 (a)), the poleward population moves southward, and the two ULF populations become indistinguishable from each other. This, as will be discussed below, fits well into the expected dipole tilt control over cusp latitude.





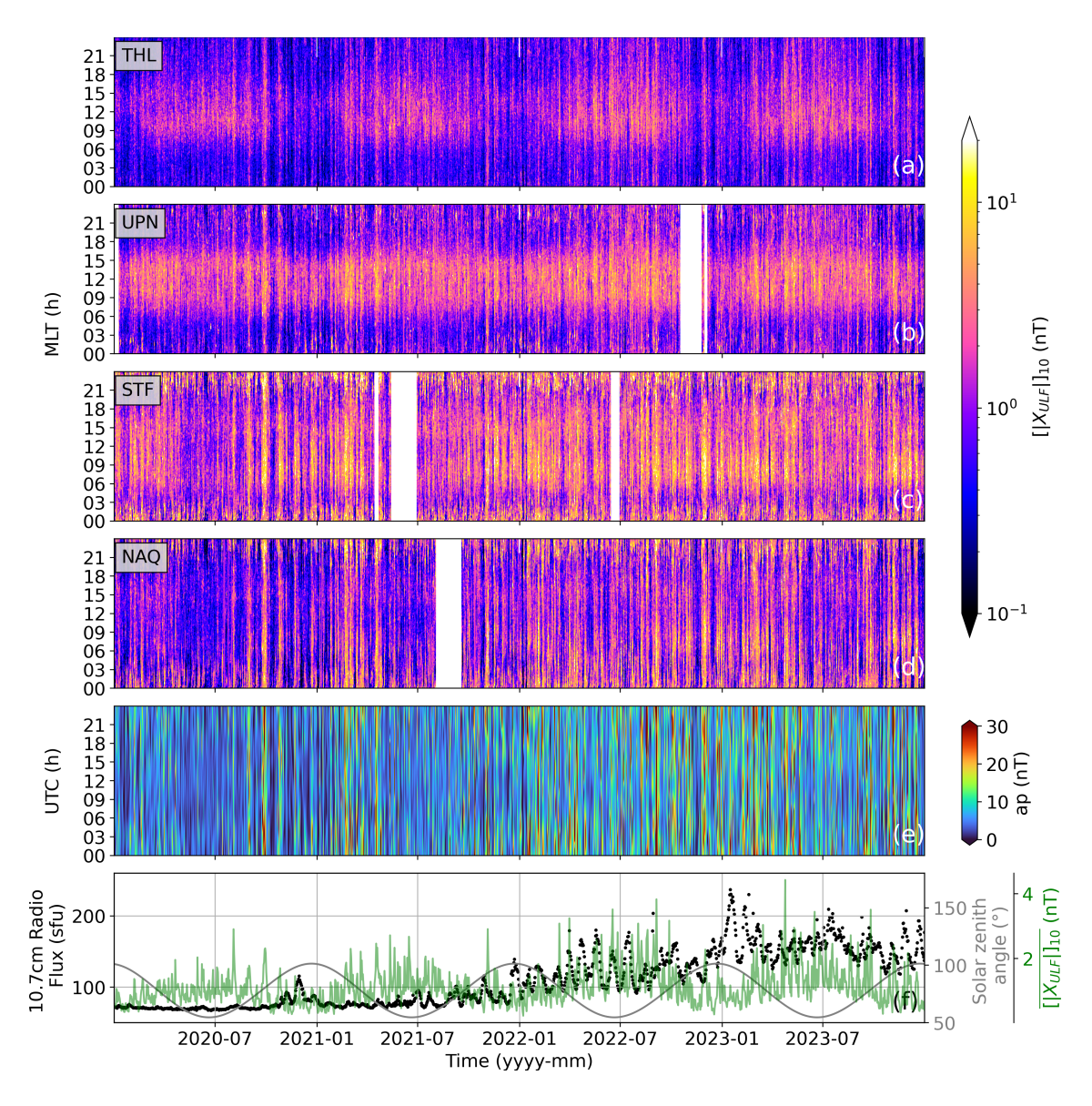


**Figure 1.** (a)–(d): ULF signals at the four stations THL, UPN, STF, and NAQ for four years, as a function of MLT. (e): Geomagnetic activity *ap* index as a function of UTC. (f): The daily average ULF signal measured at THL (green), the solar zenith angle (grey), and the daily solar flux F10.7 (black).

## 105 4 Interpretation and discussion

The results presented in Fig. 2 reveal some systematic features. At the two northernmost stations, there is primarily ULF activity centered on magnetic noon, while moving southwards, the situation changes to the opposite, with the bulk of activity occurring during nighttime. This can easily be understood by the diurnal variation in these stations' location with respect to



120

125

130

135

140



the auroral oval and associated geophysical processes. Around nighttime, THL is located deep in the polar cap, with magnetic field lines mapping to the magnetospheric lobes and far into the magnetotail, far away from the auroral oval, while at noon, the station will be closer to the cusp footprint with fieldlines mapping to the magnetopause.

UPN is somewhat similar to THL; both are closer to cusp latitudes than the nightside auroral oval. At STF, we clearly see the presence of ULF activity around midnight; this station is close enough to the auroral oval that the poleward expansion associated with the substorm expansion phase will reach this latitude. The presence of ULF waves in conjunction with the establishment of the substorm current wedge and upward Birkeland current is well studied in the literature. Although we still see a signal around noon at STF, it is split into two local maxima with a local minimum at noon. This can be explained by the station being briefly subauroral, but encounters the oval at fairly late and early hours around noon. The ULF waves associated with this double hump may then be attributed to *travelling convection vortex* (TCV) activity (Friis-Christensen et al., 1988), where irregularities/pressure transients along the magnetospheric flanks create sets of Birkeland currents that move along the poleward edge (i.e., the part that maps to the equatorial magnetopause) of the auroral oval in an anti-sunward direction.

At NAQ, which is in the nightside auroral oval, only the nightside, substorm-related ULF waves are seen. Generally, the effect of geomagnetic storms is seen at all stations, where the ULF activity lasts throughout the whole day. The combination of enhanced solar wind magnetosphere coupling, as well as enhanced electrojet power and substorm activity, is clearly seen in the *ap* index.

Another striking feature is the seasonal variation, which increases towards high latitudes. Using the empirical formulas found by Moen and Brekke (1993), we calculated the Hall conductance above the same stations as those presented in Fig. 1. Assuming that the conductivity is not modulated by particle precipitation, the formulas take solar zenith angle and solar luminosity, using F10.7 as a proxy, into account. The resulting Hall conductances, presented in Fig. 4, show great similarity with the ULF power plots of Fig. 1, especially at THL; variations in F10.7 appear as vertical lines where this value peaks, and all are constrained by the solar zenith angle, only producing values when the Sun is above the horizon. Considering that the ground magnetic ULF signals are caused by horizontal ionospheric currents, which depend on electric fields and ionospheric conductivity (Ohm's law); the Figure illustrates that presence of EUV from the Sun is a prerequisite to produce the observed ULF signals in the case where particle precipitation is not energetic enough to enhance electron density (conductivity) in the ionospheric *E-region*. This is the case on open magnetic field lines in the cusp. Furthermore, the similarity between the conductivity plots and ULF power plots at THL and UPN indicates that a varying ionospheric electric field generates the observed magnetic ULF signal.

The situation is somewhat different when moving southward. Here, the similarity to the conductivity plot disappears, and there are distinct periods where the ULF waves occur outside the region of high solar-induced conductivities, which is an indication of modulation in the conductivity by particle precipitation (potentially in concert with fluctuating electric fields). The distribution of signals at STF, which is at a latitude comparable to the Antarctic South Pole Station, is in very good accordance with the study of Motoba et al. (2019) where their ULF observations were accompanied by observed > 1 keV electron precipitation and by modulations in auroral brightness, which again is a strong indicator of particle precipitation. The presence of > 1 keV electrons is a strong indicator of particle precipitation on closed magnetic field lines and, thus, dynamics associated with sub-cusp particle populations. This underscores the fact that the ULF waves observed at STF, which could, in



150

155

165

170

175



general terms, be categorized as dayside, high latitude ULF signals, mainly belong to a different mechanism compared to what is observed further poleward at UPN and THL.

As was shown by Rostoker et al. (1972), there are two populations of ULF signatures on the dayside, although for somewhat lower but overlapping frequencies than studied here. One is a fairly narrow band which increases in frequency by decreasing magnetic latitude – as expected for Alfvén waves bouncing between hemispheres – and the other, wideband, above  $\sim 75^{\circ}$  magnetic latitude, which cannot be explained by bouncing Alfvén waves. The two populations converge just below  $75^{\circ}$  magnetic latitude, and therefore, a station here would most likely see a mixture of both populations.

Figure 2 shows clearly that there is a local minimum around 75° QD-latitude. Following the results of Anderson and Bukowski (2024) related to dipole tilt effect on cusp latitude, we find that the average equatorward edge of the (northern hemisphere) MLT noon cusp at 15 UT will be about 80° QD-latitude during summer and 77° QD-latitude during winter solstice. The statistical cusp equatorward boundaries are indicated as white dashed lines in the Figure. It should be noted here that we expect the seasonal motion of the cusp, associated with the dipole tilt, to contribute to the seasonal variation seen in Fig. 1, in particular at THL, which will be about 6° north of the cusp equatorward boundary during winter solstice. This is furthermore confirmed by the disappearance of the  $\sim 75^{\circ}$  minimum in winter. The movement of the poleward ULF population is in accordance with the polar cusp movement (Anderson and Bukowski, 2024), suggesting the ULF signatures are generated by cusp processes. Figure 2 also supports this notion since intense ULF signatures are more dominant further north during  $\theta_c = 0^{\circ}$  and  $\theta_c = \pm 45^{\circ}$ , i.e. when  $B_z > 0$ , which mirrors the poleward movement of the cusp during those IMF conditions, (e.g. Newell et al., 1989; Johnsen and Lorentzen, 2012). No distinct cusp signature was identified by Engebretson et al. (1995), while Pilipenko et al. (2015) reported on ULF signatures occurring several degrees south of the equatorward cusp boundary. However, most of the data analysed in Engebretson et al. (1995), and all of the data in Pilipenko et al. (2015), were collected during winter. As shown in Fig. 3, the two ULF populations tend to merge and become indistinguishable in winter, which may explain why dayside ULF signatures are observed much farther equatorward than the expected cusp boundary, by these authors. The findings by e.g. Johnsen and Lorentzen (2012) show that the latitude of the OCB in the cusp is relatively stable during IMF northward conditions, but moves southwards during increasing negative values (by about  $0.5^{\circ}$  per IMF  $B_z$  nT). Thus, we would expect an ULF signal associated with the cusp to be fairly constrained towards northern latitudes, while its latitude towards the south would be more dynamic as a function of negative IMF  $B_z$  values and to be smeared out in our statistical treatment (in Fig. 3). In light of this, it is no surprise that the identified noon-time, northern ULF signal also exists south of the indicated statistical equatorward boundary of the cusp (horizontal, white, dashed line). We conclude that the observed ULF signals centered on noon are, indeed, associated with open cusp field lines. The dayside ULF signals seen further southward are, as discussed above, the ones described in the study by Motoba et al. (2019), which are related to more energetic particle precipitation than expected for the cusp. The presence of a minimum between the northern and southern ULF signals at noon during summer, and the fact that they differ in their seasonal dependency (i.e., solar or precipitation produced conductivity and different response to changes in dipole tilt), indicates that different dynamic processes are at play.

The signal north of 75° QD-latitude is a separate population of dayside ULF waves associated with dynamics on open magnetic field lines, which has not, to the best of our knowledge, been identified or isolated before. The existence of the local



180

185

190

195

200

205

210



minimum at 75° QD-latitude, and the poleward ULF signals' dependence on solar illumination, strongly indicates that this signal has a different source than the ones to the south. The MLT constraint of about 7 – 17 also indicates that this is a pure dayside phenomenon associated with dynamics at the magnetopause, regardless of IMF orientation. Especially at very high latitudes (at THL), the physical distance along the Sun-Earth line between magnetic noon and midnight is small; the absence of ULF waves close to magnetic midnight at this latitude indicates that the ionosphere above the station stops receiving ULF waves when the local magnetic field lines start convecting into the interior magnetosphere/mantle.

Figure 2 shows, as mentioned above, that the northern ULF signal around noon exists for all clock angles, indicating that the generating mechanism of the corresponding ULF waves does not favour subsolar or lobe reconnection. Nightside ULF activity at relatively low latitudes is stronger during southward IMF, as expected for substorm activity. For clock angles of  $\pm 90^{\circ}$ , i.e. when the IMF  $B_y$  dominates over  $B_z$ , the bulk of high latitude ULF activity moves towards post/pre noon. This is very much in accordance with the notion of how the magnetopause location of the reconnection X-lines moves with IMF  $B_y$ , and underpins that the ULF waves actually are on open field lines.

Kozyreva et al. (2019) suggest that Pc 5 pulsations observed above Svalbard are related to magnetopause processes, but cannot exclude "the possibility that the observed ULF signature is caused by heavily damped Alfvenic oscillations of the last closed field lines". The cusp aurora is located north of zenith and accompanied by a green-dominated aurora to the south in the cases presented by these authors, with the highest power of their Pc 5 signal south of their obtained OCB. During winter conditions, the expected ULF signal on open field lines is weak, as discussed above and shown in Fig. 1 and 4. Considering that only one or two magnetometer stations constitute their ULF observations north of the OCB and that Rostoker et al. (1972) shows that the two different types of ULF waves converge near the cusp, we are inclined to support their suspicion of Alfvenic oscillations on closed field lines, which is very similar to the observations by Motoba et al. (2019). Our results represent higher temporal resolution, but considering the broadband nature of the dayside high latitude ULF signals, on the other hand, do show a clear presence of ULF waves on open magnetic field lines. This lends a hand to the argumentation by Kozyreva et al. (2019) in support of magnetopause surface waves.

Although being outside the scope of this study, it is tempting to briefly mention the source mechanism in the magnetosphere for these cusp ULF waves. There is a wide range of magnetopause or polar cusp region processes that might give rise to observed ULF waves in the cusp (e.g. Glassmeier, 1989). We notice, as was also pointed out by Vennerstrøm (1999), that there is also a ULF signal strength dependence on solar wind velocity, which might point towards both enhanced magnetopause reconnection rates, but also towards stronger flow shears in the exterior of the cusp. The pulsed injection of plasma through the cusp by *flux transfer events* (FTEs), with a repetition rate between a few to about 15 minutes (Lockwood and Wild, 1993), and the role of multiple reconnection *X*-lines theorised by Lee et al. (1988) and observed e.g. by Hasegawa et al. (2010) and Fuselier et al. (2022), makes a very convincing basis for Kelvin-Helmholtz instability, owing to flow shears in the cusp inflow region, giving rise to a wide band ULF signal. The correlation of nightside FTEs and Pi 2 waves in the magnetospheric lobe (Keiling et al., 2006), furthermore, lends credibility to this notion.

The observed seasonal variation in the ULF signal at high latitudes depends on the Hall conductivity, i.e., the waves incident on the ionosphere will create a Hall current in the ionospheric *E-region*, generating ULF magnetic signals at ground. If the Hall





215 This means that, even though not driving a current, the wave activity will drive an alternating **E** × **B** motion in the *F-region*. We already know that FTEs generate *reversed flow events* (RFEs) in the cusp (Rinne et al., 2007), and these, together with polar cap patches, have been shown to accompany significant phase scintillations on *Global Navigation Satellite System* (GNSS) signals, indicating the generation of small-scale electron density irregularities through e.g., ionospheric Kelvin-Helmholtz instability (Spicher et al., 2020). We therefore speculate that the ULF waves incident on the cusp, even though not visible from the ground owing to seasonal variation in the Hall conductivity, but still being present as ULF alternating electric fields, might be the necessary perturbing force seeding such instabilities.

#### 5 Conclusions

225

230

In this work, we show for the first time the existence of an isolated population of ULF waves at cusp latitudes, which are most likely on open magnetic field lines or associated with cusp dynamics and separated from other dayside ULF waves. This result contrasts with earlier investigations, which concluded that there are no identifiable cusp ULF waves on open field lines, but rather a population located in the vicinity of the cusp. However, earlier investigations have focused on winter conditions, which is likely the reason for their conclusions. We find that the cusp ULF population crystallizes out of the data during the summer months. This can be explained by the combination of the following points:

- During the summer period, Earth's dipole axis tilts toward the Sun, which pushes the dayside OCB, i.e., the cusp, to higher latitudes (see e.g. Anderson and Bukowski (2024)). This moves it away from the equatorward dipole-like field lines that contain standing Alfvenic waves that bounce between the hemispheres (Pi 2 waves), which have their source from substorms in the nightside and other internal magnetospheric processes. Our study shows a clear minimum in ULF signal activity around 75° QD-latitude during summer, which separates ULF signals at cusp latitudes from those at relatively lower latitudes.
- Electron precipitation in the cusp, which originates from the magnetosheath, is very soft, typically below 500 eV. With such low energies, energy is deposited in the *F-region* above, say 200 km, rather than lower in the ionosphere. This will inhibit this precipitation to modulate Hall and Pedersen conductivities in the *E-region*. Therefore, the ULF signatures observed on the ground, which are the result of alternating/oscillating Hall currents in the *E-region*, are the result of an alternating *E-field*, rather than an alternating conductivity. In order for this *E-field* to modulate currents in the *E-region*, the conductivity as produced by solar EUV needs to be sufficiently high, a condition which is only achieved during the summer months.

Although tempting to combine dayside auroral observations with ULF ground-based measurements to investigate their relationship, it proves impossible since one requires complete darkness (winter conditions), while the other requires sunlight (summer conditions). However, there is no reason that the *E-fields* driving the observed ULF waves during summer are not



255

260

265

270



245 present during winter. Dedicated high cadence radar and/or satellite measurements would reveal this and should be attempted in the future.

An interesting feature of our identified cusp ULF population is that its presence does not rely on the IMF orientation. Both for northward and southward IMF conditions, it is clearly present, while the population immediately equatorward is much clearer during southward IMF. IMF  $B_y$  modulates the MLT location, with the bulk of ULF signatures on the morning (evening) side of magnetic noon for  $B_y < 0 \ (> 0)$ , this is in accordance with the cusp convection throat region (Svalgaard-Mansurov effect (Svalgaard, 1968; Mansurov, 1969; Newell et al., 2004)), location of cusp precipitation (Newell and Meng, 1989), motion of *poleward moving auroral forms* (PMAFs) (Sandholt and Farrugia, 1999), and DPY behaviour (Friis-Christensen and Wilhjelm, 1975), which again confirms the notion of dealing with a cusp related ULF population. We also observe that the dayside equatorward (sub-cusp) ULF population has a minimum at magnetic local noon, most likely due to TCVs and associated Birkeland currents, which are generated along the flanks of the magnetosphere, away from the bow-shock nose.

The presence of FTEs, of which signatures are a common phenomenon in the cusp, and that have also been associated with ULF waves related to magnetotail reconnection, is an attractive candidate for ULF wave generation in the cusp. FTEs have earlier been established to create PMAFs and reversed flow events. These are believed to be strongly associated with the generation of polar cap patches and motion of high density plasma into the polar cap, giving rise to strong electron density gradients with consequential plasma instability driven generation of small-scale irregularities, which again create scintillations on satellite communication and GNSS signals. For instance, Spicher et al. (2020) gives a convincing case for the creation of such irregularities from Kelvin-Helmholtz instabilities generated by an RFE in the cusp, and thus an FTE event. We speculate that the necessary perturbation needed to allow such instabilities to start growing can be attributed to ULF waves as identified in this work, which may be associated with the same FTEs. This should be investigated in the future by applying both ground-based magnetometers, radar systems, and satellite measurements, preferably in the summer hemisphere.

Data availability. The magnetic data used in this paper are available by request at DTU Space.

Author contributions. MVE performed the data analysis, generated all the figures, and wrote parts of and coordinated the evolution of the manuscript. MGJ interpreted the results and wrote most of the manuscript. NO initiated the study, supervised the work, and provided feedback on the manuscript. MVE, MGJ, and NO all contributed to the discussion of the results and the final editing of the manuscript. ANW provided the magnetic data and gave feedback on the manuscript. All authors have read and approved the manuscript.

Competing interests. The authors declare that they have no conflict of interest.



275

280



Acknowledgements. We are grateful to the Space Weather Forecasting for Arctic Defence Operations (SWADO) team at DTU Space for providing the magnetic data and operating the magnetometer stations in Greenland. The authors also thank the Danish Ministry of Defence Acquisition and Logistics Organisation (DALO) for funding the research presented in this paper. The magnetic data used in this paper are available for request at DTU Space.

We thank the providers of the F10.7, Dst, ap, and SML indices that enabled the analysis presented in this paper. The F10.7 index was provided by the National Research Council Canada, in partnership with Natural Resources Canada, and obtained via https://www.spaceweather.gc.ca/forecast-prevision/solar-solaire/solarflux/sx-5-en.php, the Dst index was provided by the WDC for Geomagnetism, Kyoto (https://wdc.kugi.kyoto-u.ac.jp/wdc/Sec3.html, Nose et al. (2015)), and the ap index was provided by GFZ (Matzka et al., 2021a, b). We gratefully acknowledge the SuperMAG collaborators (https://supermag.jhuapl.edu/info/?page=acknowledgement) for the use of the SML index (Newell and Gjerloev, 2011).

OMNI data were obtained via GSFC/SPDF OMNIweb (https://omniweb.gsfc.nasa.gov/form/omni\_min.html). We thank the ACE MAG and SWEPAM instrument teams, the ACE Science Center, the DSCOVR PlasMag instrumentation team, and the Wind MFI and SWE instrument teams for providing the ACE, DSCOVR, and Wind data.





#### 285 References

290

- Anderson, P. C. and Bukowski, A. L.: Magnetic Local Time and Interplanetary Magnetic Field By Variation of Cusp Location Dependence on Dipole Tilt, Journal of Geophysical Research: Space Physics, 129, https://doi.org/10.1029/2023ja031886, 2024.
- Engebretson, M. J., Hughes, W. J., Alford, J. L., Zesta, E., Cahill, L. J., Arnoldy, R. L., and Reeves, G. D.: Magnetometer array for cusp and cleft studies observations of the spatial extent of broadband ULF magnetic pulsations at cusp/cleft latitudes, Journal of Geophysical Research: Space Physics, 100, 19 371–19 386, https://doi.org/10.1029/95ja00768, 1995.
- Engebretson, M. J., Posch, J. L., Pilipenko, V. A., and Chugunova, O. M.: ULF waves at very high latitudes, pp. 137–156, American Geophysical Union, https://doi.org/10.1029/169gm10, 2006.
- Eschenhagen, M.: On minute, rapid, periodic changes of the Earth's magnetism, Terrestrial Magnetism, 2, 105–114, https://doi.org/10.1029/tm002i003p00105, 1897.
- Feldstein, Y. and Starkov, G.: Dynamics of auroral belt and polar geomagnetic disturbances, Planetary and Space Science, 15, 209–229, https://doi.org/10.1016/0032-0633(67)90190-0, 1967.
  - Friis-Christensen, E. and Wilhjelm, J.: Polar cap currents for different directions of the interplanetary magnetic field in the Y-Z plane, Journal of Geophysical Research, 80, 1248–1260, https://doi.org/10.1029/ja080i010p01248, 1975.
- Friis-Christensen, E., McHenry, M. A., Clauer, C. R., and Vennerstrøm, S.: Ionospheric traveling convection vortices observed near the polar cleft: A triggered response to sudden changes in the solar wind, Geophysical Research Letters, 15, 253–256, https://doi.org/10.1029/gl015i003p00253, 1988.
  - Fuselier, S. A., Kletzing, C. A., Petrinec, S. M., Trattner, K. J., George, D., Bounds, S. R., Sawyer, R. P., Bonnell, J. W., Burch, J. L., Giles, B. L., and Strangeway, R. J.: Multiple Reconnection X-Lines at the Magnetopause and Overlapping Cusp Ion Injections, Journal of Geophysical Research (Space Physics), 127, e30354, https://doi.org/10.1029/2022JA030354, 2022.
- Glassmeier, K. H.: ULF pulsations in the polar cusp and cap, in: Electromagnetic Coupling in the Polar Clefts and Caps, edited by Sandholt, P. E. and Egeland, A., p. 167, 1989.
  - Greenstadt, E. W., Inouye, G. T., Green, I. M., and Judge, D. L.: Vela 3 magnetograms at  $18~R_E$  structure and pulsations in the magnetosheath, Journal of Geophysical Research, 72, 3855–3876, https://doi.org/10.1029/jz072i015p03855, 1967.
- Harang, L.: Observations of micropulsations in the magnetic records at Tromsø, Terrestrial Magnetism and Atmospheric Electricity, 37, 57, https://doi.org/10.1029/TE037i001p00057, 1932.
  - Hasegawa, H., Wang, J., Dunlop, M. W., Pu, Z. Y., Zhang, Q. H., Lavraud, B., Taylor, M. G. G. T., Constantinescu, O. D., Berchem, J., Angelopoulos, V., McFadden, J. P., Frey, H. U., Panov, E. V., Volwerk, M., and Bogdanova, Y. V.: Evidence for a flux transfer event generated by multiple X-line reconnection at the magnetopause, Geophys. Res. Lett., 37, L16101, https://doi.org/10.1029/2010GL044219, 2010.
- Heppner, J. P., Sugiura, M., Skillman, T. L., Ledley, B. G., and Campbell, M.: OGO-A magnetic field observations, Journal of Geophysical Research, 72, 5417–5471, https://doi.org/10.1029/jz072i021p05417, 1967.
  - Holzworth, R. H. and Meng, C.: Mathematical representation of the auroral oval, Geophysical Research Letters, 2, 377–380, https://doi.org/10.1029/gl002i009p00377, 1975.
- Jacobs, J. A., Kato, Y., Matsushita, S., and Troitskaya, V. A.: Classification of geomagnetic micropulsations, Journal of Geophysical Research, 69, 180–181, https://doi.org/10.1029/jz069i001p00180, 1964.



325

330

340

355



- Johnsen, M. G. and Lorentzen, D. A.: A statistical analysis of the optical dayside open/closed field line boundary, Journal of Geophysical Research: Space Physics, 117, https://doi.org/10.1029/2011ja016984, 2012.
- Keiling, A., Fujimoto, M., Hasegawa, H., Honary, F., Sergeev, V., Semenov, V. S., Frey, H. U., Amm, O., Rème, H., Dandouras, I., and Lucek, E.: Association of Pi2 pulsations and pulsed reconnection: ground and Cluster observations in the tail lobe at 16 R<sub>E</sub>, Annales Geophysicae, 24, 3433–3449, https://doi.org/10.5194/angeo-24-3433-2006, 2006.
- Kepko, L. and Kivelson, M.: Generation of Pi2 pulsations by bursty bulk flows, Journal of Geophysical Research: Space Physics, 104, 25 021–25 034, https://doi.org/10.1029/1999ia900361, 1999.
- Kozyreva, O., Pilipenko, V., Lorentzen, D., Baddeley, L., and Hartinger, M.: Transient Oscillations Near the Dayside Open-Closed Boundary: Evidence of Magnetopause Surface Mode?, Journal of Geophysical Research: Space Physics, 124, 9058–9074, https://doi.org/10.1029/2018ja025684, 2019.
- Lee, L. C., Shi, Y., and Lanzerotti, L. J.: A mechanism for the generation of cusp region hydromagnetic waves, J. Geophys. Res., 93, 7578–7585, https://doi.org/10.1029/JA093iA07p07578, 1988.
- Lockwood, M. and Wild, M. N.: On the quasi-periodic nature of magnetopause flux transfer events, J. Geophys. Res., 98, 5935–5940, https://doi.org/10.1029/92JA02375, 1993.
- Mansurov, S. M.: New evidence of the relationship between magnetic field in space and on the Earth, Geomagn. Aeron., pp. 768–773, 1969.

  Matzka, J., Bronkalla, O., Tornow, K., Elger, K., and Stolle, C.: Geomagnetic Kp index, https://doi.org/10.5880/KP.0001, 2021a.
  - Matzka, J., Stolle, C., Yamazaki, Y., Bronkalla, O., and Morschhauser, A.: The Geomagnetic Kp Index and Derived Indices of Geomagnetic Activity, Space Weather, 19, https://doi.org/10.1029/2020sw002641, 2021b.
  - McHarg, M. G. and Olson, J. V.: Correlated optical and ULF magnetic observations of the winter cusp Boundary layer system, Geophysical Research Letters, 19, 817–820, https://doi.org/10.1029/92g100117, 1992.
  - McHarg, M. G., Olson, J. V., and Newell, P. T.: ULF cusp pulsations: Diurnal variations and interplanetary magnetic field correlations with ground-based observations, Journal of Geophysical Research: Space Physics, 100, 19729–19742, https://doi.org/10.1029/94ja03054, 1995.
- Moen, J. and Brekke, A.: The solar flux influence on quiet time conductances in the auroral ionosphere, Geophysical Research Letters, 20, 971–974, https://doi.org/10.1029/92gl02109, 1993.
  - Motoba, T., Ebihara, Y., Ogawa, Y., Kadokura, A., Engebretson, M. J., Angelopoulos, V., Gerrard, A. J., and Weatherwax, A. T.: On the Driver of Daytime Pc3 Auroral Pulsations, Geophysical Research Letters, 46, 553–561, https://doi.org/10.1029/2018gl080842, 2019.
  - Newell, P. T. and Gjerloev, J. W.: Evaluation of SuperMAG auroral electrojet indices as indicators of substorms and auroral power, Journal of Geophysical Research: Space Physics, 116, https://doi.org/10.1029/2011ja016779, 2011.
- Newell, P. T. and Meng, C.-I.: Dipole tilt angle effects on the latitude of the cusp and cleft/low-latitude boundary layer, Journal of Geophysical Research: Space Physics, 94, 6949–6953, https://doi.org/https://doi.org/10.1029/JA094iA06p06949, 1989.
  - Newell, P. T., Meng, C., Sibeck, D. G., and Lepping, R.: Some low-altitude cusp dependencies on the interplanetary magnetic field, Journal of Geophysical Research: Space Physics, 94, 8921–8927, https://doi.org/10.1029/ja094ia07p08921, 1989.
  - Newell, P. T., Ruohoniemi, J. M., and Meng, C.: Maps of precipitation by source region, binned by IMF, with inertial convection streamlines, Journal of Geophysical Research: Space Physics, 109, https://doi.org/10.1029/2004ja010499, 2004.
  - Nose, M., Iyemori, T., Sugiura, M., Kamei, T., Matsuoka, A., Imajo, S., and Kotani, T.: Geomagnetic Dst index, World Data Center for Geomagnetism, Kyoto, https://doi.org/10.17593/14515-74000, 2015.





- Pilipenko, V., Belakhovsky, V., Engebretson, M. J., Kozlovsky, A., and Yeoman, T.: Are dayside long-period pulsations related to the cusp?, Annales Geophysicae, 33, 395–404, https://doi.org/10.5194/angeo-33-395-2015, 2015.
- 360 Richmond, A. D.: Ionospheric Electrodynamics Using Magnetic Apex Coordinates, J. Geomagn. Geoelectr., 47, 191–212, https://doi.org/10.5636/jgg.47.191, 1995.
  - Rinne, Y., Moen, J., Oksavik, K., and Carlson, H. C.: Reversed flow events in the winter cusp ionosphere observed by the European Incoherent Scatter (EISCAT) Svalbard radar, Journal of Geophysical Research (Space Physics), 112, A10313, https://doi.org/10.1029/2007JA012366, 2007.
- 365 Rolf, B.: Giant micropulsations at Abisko, Terrestrial Magnetism and Atmospheric Electricity, 36, 9, https://doi.org/10.1029/TE036i001p00009, 1931.
  - Rostoker, G., Samson, J. C., and Higuchi, Y.: Occurrence of Pc 4, 5 micropulsation activity at the polar cusp, J. Geophys. Res., 77, 4700–4706, https://doi.org/10.1029/JA077i025p04700, 1972.
- Sakurai, T. and McPherron, R. L.: Satellite observations of Pi 2 activity at synchronous orbit, Journal of Geophysical Research: Space Physics, 88, 7015–7027, https://doi.org/10.1029/ja088ia09p07015, 1983.
  - Sandholt, P. E. and Farrugia, C. J.: On the dynamic cusp aurora and IMF By, Journal of Geophysical Research: Space Physics, 104, 12461–12472, https://doi.org/10.1029/1999ja900126, 1999.
  - Sonett, C. P., Judge, D. L., and Kelso, J. M.: Evidence concerning instabilities of the distant geomagnetic field: Pioneer I, Journal of Geophysical Research, 64, 941–943, https://doi.org/10.1029/jz064i008p00941, 1959.
- Sonnerup, B. U. Ö., Cahill, L. J., and Davis, L. R.: Resonant vibration of the magnetosphere observed from Explorer 26, Journal of Geophysical Research, 74, 2276–2288, https://doi.org/10.1029/ja074i009p02276, 1969.
  - Spicher, A., Deshpande, K., Jin, Y., Oksavik, K., Zettergren, M. D., Clausen, L. B. N., Moen, J. I., Hairston, M. R., and Baddeley, L.: On the Production of Ionospheric Irregularities Via Kelvin-Helmholtz Instability Associated with Cusp Flow Channels, Journal of Geophysical Research (Space Physics), 125, e27734, https://doi.org/10.1029/2019JA027734, 2020.
- Svalgaard, L.: Sector structure of the interplanetary magnetic field and daily variation of the geomagnetic field at high latitudes, Danish Meteorlogical Institute, Geophysical Papers, Preprint R-6, 1968.
  - Vennerstrøm, S.: Dayside magnetic ULF power at high latitudes: A possible long-term proxy for the solar wind velocity?, Journal of Geophysical Research: Space Physics, 104, 10145–10157, https://doi.org/10.1029/1999ja900015, 1999.





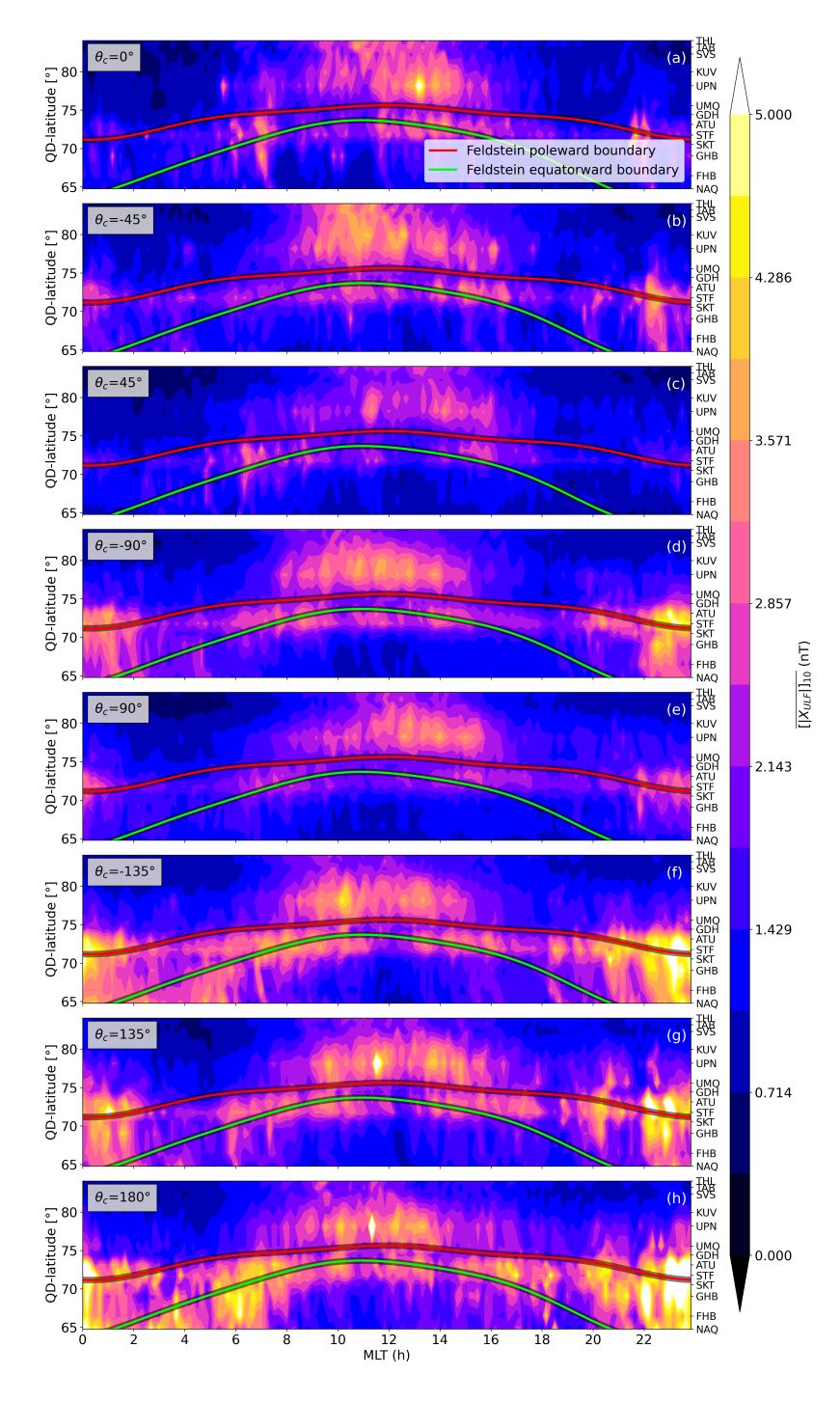


**Figure 2.** Average ULF signature amplitudes during summer (May–July) in 2020–2023 for the Greenland west-coast magnetometer chain (station ID given on the right y-axis) with respect to QD-latitude and MLT for different IMF clock angles. The equatorward (green curve) and poleward (red curve) boundaries of the auroral oval are computed with the Feldstein model.





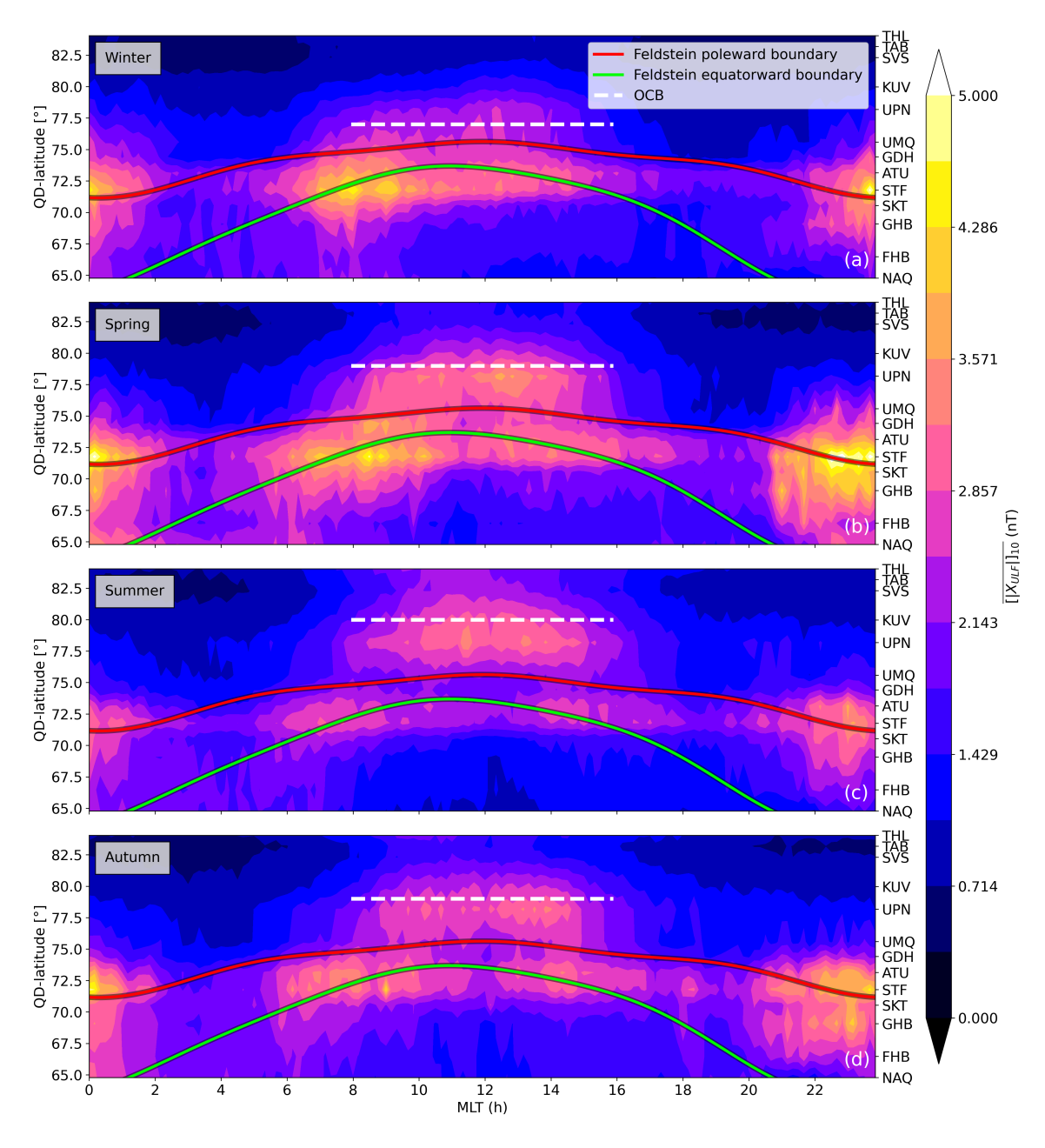


**Figure 3.** MLT vs. QD-latitude of the mean 10-minute average ULF signature amplitudes in 2020–2023 sectioned into the seasons (a) winter (Nov–Jan), (b) spring (Feb–Apr), (c) summer (May–Jul), and (d) autumn (Aug–Oct). The station ID is given on the right y-axis. The poleward (red curve) and equatorward (green curve) boundaries of the auroral oval as given by the Feldstein model. The white dashed line represents the corresponding cusp equatorward boundary (OCB) for the interval 11.50 – 12.50 MLT (displayed from 8 – 16 MLT) determined using the method of Anderson and Bukowski (2024).



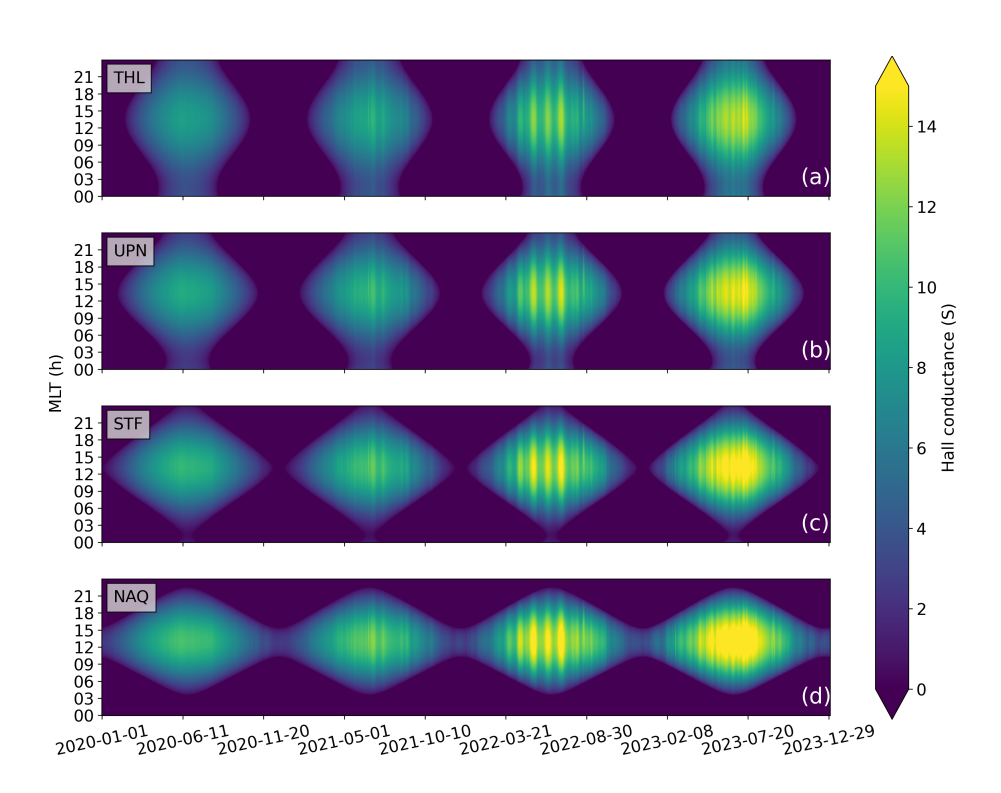


**Figure 4.** Hall conductances at four stations, (a) THL, (b) UPN, (c) STF, and (d) NAQ, as given by the empirical formula of Moen and Brekke (1993), throughout four years, where the y-axis is given in MLT.